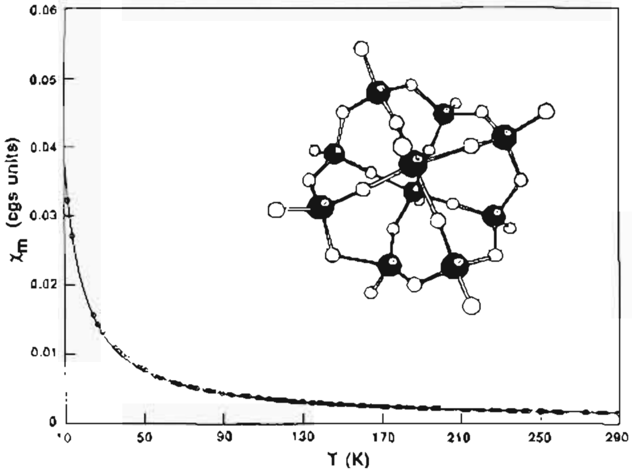

Figure 2. Plot of molar susceptibility for **1** from 10 to 290 K. The open circles are data; the line is the best fit to the Van Vleck equation (see text). Also shown is the structure of the $V_{10}O_{26}^{4-}$ ion (V^{IV}–V^{IV} = 4.44 Å).[4b]

decomposed the cluster to give the same uncharacterizable mixture. This behavior was somewhat unexpected, considering that many polyoxoanion structures are stable to oxidation or reduction.[9] It is interesting to note that the well-known[10] $H_3V_{10}O_{28}^{3-}$ displays irreversible reduction chemistry, at least in acetonitrile solution.

The solution ESR spectrum of $V_{10}O_{26}^{4-}$ reported by Heitner-Wirguin and Selbin shows a 15-line pattern with $a(^{51}V)$ = 102 G, consistent with coupling to two equivalent ^{51}V nuclei ($I = {}^7/_2$). In order for two d^1 centers to give rise to this type of pattern, the coupling between the triplet and singlet electronic states must be at least a great as the hyperfine coupling in the ESR spectrum (~0.01 cm^{-1} at 9.5 GHz).[11] With this in mind, we undertook a thorough investigation of the magnetic properties of the compound. Figure 2 shows data for corrected molar susceptibility (χ_m^{corr}) as a function of temperature; superimposed is the best-fit curve for the susceptibility derived from the Van Vleck equation (eq 2),[12] which assumes an interaction of the form $\mathcal{H} = -2JS_1\cdot S_2$.

$$\chi = \frac{Ng^2\beta^2}{3kT}\left[1 + \frac{1}{3}\exp\left(\frac{-2J}{kT}\right)\right] + \text{TIP} \qquad (2)$$

The compound has μ_{eff} = 1.85 μ_B[13] per V^{IV} center at 293 K, perhaps suggestive of ferromagnetic coupling. The curve shown is for $2J$ = 0.9 cm^{-1}, indicating a weak ferromagnetic coupling (i.e., triplet ground state), which is ~100 times greater than the coupling necessary to rationalize the ESR spectrum. The temperature-independent paramagnetism (TIP) is estimated to be ~3 × 10^{-4} cgsu/mol, considered normal for a first-row complex.[14] Dimeric vanadyl(IV) tartrate complexes, which are structurally similar to $V_{10}O_{26}^{4-}$, also display ferromagnetic coupling;[15] however, the quality of the published data is not sufficient to allow for meaningful comparisons. To date, these are the only known ferromagnetically coupled vanadyl complexes.[16]

Acknowledgment. The authors wish to thank the Air Force Office of Scientific Research and the donors of the Petroleum Research Fund, administered by the American Chemical Society, for financial support. S.M.B. acknowledges the Shell Companies Foundation for fellowship support.

---

(9) (a) Pope, M. T. *Heteropoly and Isopoly Oxometalates*; Springer-Verlag: Berlin, 1983; Chapter 6. (b) Kozik, M.; Hammer, C. F.; Baker, L. C. W. *J. Am. Chem. Soc.* **1986**, *108*, 2748–2749. (c) Piepgrass, K.; Pope, M. T. *Ibid.* **1987**, *109*, 1586–1587.

(10) Day, V. W.; Klemperer, W. G.; Maltbie, D. J. *Ibid.* **1987**, *109*, 2991–3002.

(11) Reitz, D. C.; Weissman, S. I. *J. Chem. Phys.* **1960**, *33*, 700–704.

(12) (a) Van Vleck, J. H. *Theory of Electric and Magnetic Susceptibilities*; Oxford University Press: London, 1932; Chapter 9. (b) Ballhausen, C. J.; Liehr, A. D. *J. Am. Chem. Soc.* **1959**, *81*, 538–542.

(13) This value was corroborated by the Evans method in CH_3CN solution: μ_{eff} = 1.8 μ_B.

(14) Figgis, B. N. *Introduction to Ligand Fields*; Wiley-Interscience: New York, 1966; pp 278–289.

(15) (a) Hanson, M. V.; Smith C. B.; Carlisle, G. O. *Inorg. Nucl. Chem. Lett.* **1975**, *11*, 865–868. (b) Carlisle, G. O.; Simpson, G. D. *J. Mol. Struct.* **1975**, *25*, 219–221.

(16) One reviewer brought to our attention an example of ferromagnetically coupled V^{IV} atoms in the heteropolyanion $[\alpha\text{-}1,2,3\text{-}SiV^{IV}{}_3W_9O_{40}H_3]^{7-}$: Mossoba, M. M.; O'Connor, C. J.; Pope, M. T.; Sinn, E.; Hervé, G.; Tézé, A. *J. Am. Chem. Soc.* **1980**, *102*, 6864–6866. In this compound, the V^{IV} atoms are estimated to be separated by ~3.7 Å in adjacent corner-sharing octahedral sites of a Keggin structure. The magnitude of the ferromagnetic coupling was found to be J = 34.9 cm^{-1}, but interestingly, no magnetic interaction was found in the disubstituted analogue $[\alpha\text{-}1,2\text{-}SiV^{IV}{}_2W_{10}O_{40}]^{8-}$

Contribution from the Department of Chemistry,
University of Houston, Houston, Texas 77204-5641

Influence of Remote Substituents on the Properties of Bis(terpyridyl)ruthenium(II) Complexes

Randolph P. Thummel,* Vidyadhar Hegde,
and Yurngdong Jahng

Received June 1, 1988

In recent years considerable effort has been expended in trying to better understand the chemistry of ruthenium(II) diimine complexes. Much of this work has been directed toward the ultimate realization of an effective photoredox catalyst.[1] Two features that are important in the development of such a species are the absorption of light of useful wavelength and the existence of a sufficiently long-lived excited state to allow electron transfer to compete favorably with internal return to the ground state. In the area of $Ru(bpy)_3^{2+}$ chemistry (bpy = 2,2'-bipyridine), the primary design emphasis has focused on variation of the electronic and steric properties of the ligands to help control and modify the properties of their complexes.[2]

A ligand very closely related to bpy, which coordinates readily with ruthenium(II) in a 2:1 fashion, is 2,2':6',2''-terpyridine (tpy).[3] $Ru(tpy)_2^{2+}$ has been less widely studied primarily because its room-temperature excited-state lifetime is much shorter than that of $Ru(bpy)_3^{2+}$, although the underlying reasons for this are not clearly understood.[4] Nevertheless, tpy complexes are of fundamental interest for several reasons. These complexes exhibit a symmetry different from that of analogous bpy complexes. Substitution at the 4'-position of tpy does not alter the symmetry of a $Ru(tpy)_2^{2+}$ complex, while monosubstitution on a bpy ligand

---

(1) (a) Juris, A.; Balzani, V.; Barigellati, F.; Campagna, S.; Belser, P.; von Zelewsky, A. *Coord. Chem. Rev.* **1988**, *84*, 85. (b) Kalyanasundaram, K. *Coord. Chem. Rev.* **1982**, *46*, 159. (c) Watts, R. J. *J. Chem. Educ.* **1983**, *60*, 834. (d) Bignozzi, C. A.; Chiorboli, C.; Indelli, M. T.; Scandola, M. A. R.; Varani, G.; Scandola, F. *J. Am. Chem. Soc.* **1986**, *108*, 7872. (e) Abruna, H. D.; Teng, A. Y.; Samuels, G. J.; Meyer, T. J. *J. Am. Chem. Soc.* **1979**, *101*, 6745. (f) Lehn, J.-M.; Sauvage, J. P.; Ziessel, R. *Nouv. J. Chim.* **1979**, *3*, 423. (g) Juris, A.; Barigelletti, F.; Balzani, V.; Belser, P.; von Zelewsky, A. *Isr. J. Chem.* **1982**, *22*, 87. (h) Connolly, J. S. *Photochemical Conversion and Storage of Solar Energy*; Academic Press: New York, 1981; Chapters 4 and 6 and references therein.

(2) (a) Thummel, R. P.; Lefoulon, F.; Korp, J. D. *Inorg. Chem.* **1987**, *26*, 2370. (b) Thummel, R. P.; Lefoulon, F. *Inorg. Chem.* **1987**, *26*, 675. (c) Thummel, R. P.; Decloitre, Y. *Inorg. Chim. Acta* **1987**, *128*, 245. (d) Tait, C. D.; Donohoe, R. J.; DeArmond, M. K.; Wertz, D. W. *Inorg. Chem.* **1987**, *26*, 2754. (e) Barigelletti, F.; Juris, A.; Balzani, V.; Belser, P.; von Zelewsky, A. *Inorg. Chem.* **1987**, *26*, 4115. (f) Balzani, V.; Juris, A.; Barigelletti, F.; Belser, P.; von Zelewsky, A. *Sci. Pap. Inst. Phys. Chem. Res. (Jpn.)* **1984**, *78*, 78.

(3) Constable, E. C. *Adv. Inorg. Chem. Radiochem.* **1986**, *30*, 69.

(4) Kirchhoff, J. R.; McMillan, D. R.; Marnot, P. A.; Sauvage, J.-P. *J. Am. Chem. Soc.* **1985**, *107*, 1138.

0020-1669/89/1328-3264$01.50/0

Table I. ^{1}H NMR Data for Ruthenium(II) Complexes $RuL_2(PF_6)_2$[a]

complex	H_2	H_3	H_4	H_5	$H_{3'}$	H_o[b]	H_m[b]	R	CH_2
$Ru(\mathbf{4a})_2^{2+}$	7.37	7.12	7.61			7.67	7.75	7.67	3.32/3.21
$Ru(\mathbf{4b})_2^{2+}$	7.45	7.08	7.63			7.52	7.32	2.52	3.27/3.19
$Ru(\mathbf{4c})_2^{2+}$	7.32	7.08	7.63			7.55	7.72		3.29/3.17
$Ru(\mathbf{4d})_2^{2+}$	7.42	7.09	7.62			7.30	7.09		3.26
$Ru(\mathbf{4e})_2^{2+}$	7.35	7.11	7.65			7.82	8.54		3.30/3.16
$Ru(\mathbf{5a})_2^{2+}$	7.45	7.20	7.96	8.67	9.03	8.22	7.78	7.69	
$Ru(\mathbf{5b})_2^{2+}$	7.43	7.18	7.95	8.65	9.00	8.11	7.58	2.54	
$Ru(\mathbf{5c})_2^{2+}$	7.41	7.19	7.95	8.64	8.98	8.19	7.78		

[a] At 300 MHz in CD_3CN; chemical shifts reported in ppm downfield from internal Me_4Si. All peak multiplicities were as expected. [b] H_o = phenyl proton ortho to tpy; H_m = phenyl proton meta to tpy.

disrupts the symmetry of its corresponding tris complex and leads to the potential for geometric isomerism. Furthermore, the pyridine rings in $Ru(bpy)_3^{2+}$ all bind in an equivalent fashion, while for the tpy complex the two outer pyridine rings clearly bind differently from the central one. These differences raise some interesting questions concerning the nature of ruthenium complexes of tpy as compared to those of bpy.

Experimental Section

Nuclear magnetic resonance spectra were obtained in CD_3CN on a General Electric QE-300 spectrometer operating at 300 MHz, and chemical shifts are reported in parts per million downfield from Me_4Si. Ultraviolet spectra were obtained for CH_3CN solutions on a Perkin-Elmer 330 spectrophotometer.

Cyclic voltammograms were recorded by using a BAS CV-27 voltammograph and a Houston Instruments Model 100 X-Y recorder. A three-electrode system was employed, consisting of a platinum-button working electrode, a platinum-wire auxiliary electrode, and a saturated calomel reference electrode. The reference electrode was separated from the bulk of the solution by a cracked-glass bridge filled with 0.1 M TBAP in dimethyl sulfoxide (DMSO). Deaeration of all solutions was performed by passing high-purity nitrogen over the solution while measurements were being made. Reagent grade DMSO was distilled from CaH_2 under nitrogen. The supporting electrolyte, tetra-*n*-butylammonium perchlorate (TBAP), was recrystallized from EtOAc/hexane, dried, and stored in a desiccator. Half-wave potentials were calculated as an average of the cathodic and anodic peak potentials.[5]

The bridged ligands **4a–e** were obtained according to a previously described procedure.[6] The unbridged ligands **5a–c** were prepared by the reaction of 2-acetylpyridine with the appropriate benzaldehyde derivative according to the method of Chichibabin.[7]

Preparation of Ruthenium Complexes. A mixture of 1 equiv of ruthenium(III) chloride trihydrate (Aldrich) and 2.5 equiv of the terpyridine ligand in ethanol/H_2O (1:1) was refluxed under nitrogen for 15 h. The mixture was cooled and treated with 2.5 equiv of NH_4PF_6 dissolved in a minimum amount of H_2O. The resulting precipitate was collected, dried, and chromatographed on alumina by elution with CH_3CN/toluene (3:1 to 1:1). The latter fractions afforded the complex as a red solid, which was characterized by ^{1}H NMR spectroscopy (300 MHz) (see Table I.) The ruthenium complexes of **1–3** have been described previously.[8]

Results and Discussion

The model for the emitting metal-to-ligand charge-transfer (MLCT) state that is most widely accepted today for ruthenium(II) diimine complexes involves a localized excited state.[9] In other words, charge density from the photoexcited metal center is not delocalized over all the ligands but shows distinct components for different diimine ligands, favoring those which are best able to accept negative charge. The more electronegative the ligand, the lower the energy of this MLCT state and the longer the wavelength of the absorbed light. This situation is illustrated in Figure 1 for three RuL_3^{2+} complexes where L is varied from bpy, to 2,2′-biquinoline (biq), to 2,2′-bi-1,8-naphthyridine (binap).[2a] As the electronegativity of the ligand increases, the absorption curve shifts progressively to longer wavelength.

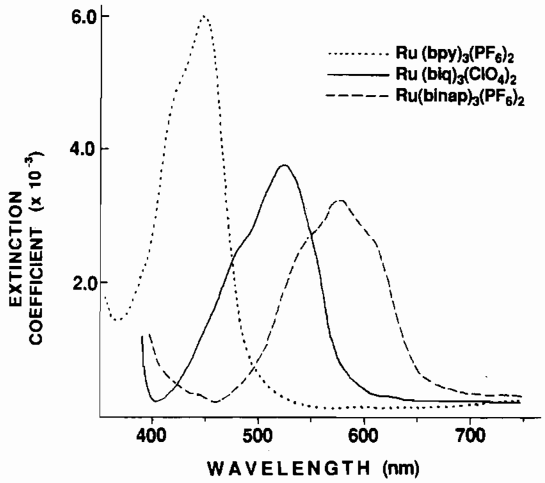

Figure 1. Electronic absorption spectra of tris(diimine)ruthenium(II) complexes (2×10^{-5} M in CH_3CN; bpy = 2,2′-bipyridine; biq = 2,2′-biquinoline; binap = 2,2′-bi-1,8-naphthyridine).[2a,b]

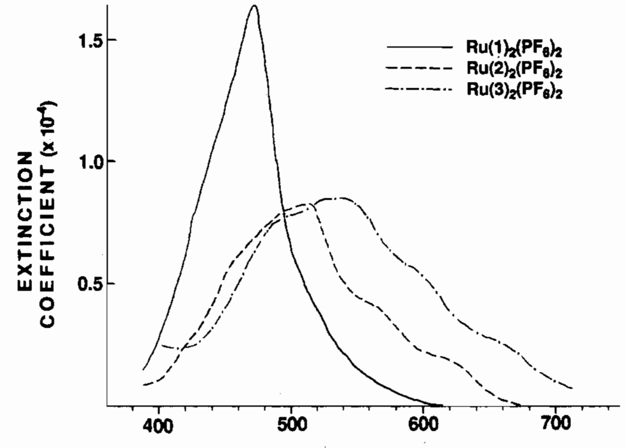

Figure 2. Electronic absorption spectra of bis(triimine)ruthenium(II) complexes (2×10^{-5} M in CH_3CN).[8]

If one considers a series of analogous terpyridine ligands, the situation is somewhat different. Figure 2 illustrates the absorption spectra for the symmetrical complexes RuL_2^{2+} where L is varied from **1** to **3**.[8] Notice that the envelope of absorption extends in a regular fashion toward longer wavelength, but the onset of absorption at shorter wavelength changes only slightly. Notice also that the absorption intensity for the tpy complex, $Ru(\mathbf{1})_3(PF_6)_2$, at its maximum is more than twice that of the other two

---

(5) Bard, A. J.; Faulkner, L. R. *Electrochemical Methods*; Wiley: New York, 1980; p 227.

(6) Hegde, V.; Jahng, Y.; Thummel, R. P. *Tetrahedron Lett.* **1987**, *28*, 4023.

(7) Frank, R. L.; Riener, E. F. *J. Am. Chem. Soc.* **1950**, *72*, 4182.

(8) Thummel, R. P.; Jahng, Y. *Inorg. Chem.* **1986**, *25*, 2527.

(9) (a) Kumar, C. V.; Barton, J. K.; Gould, I. R.; Turro, N. J.; van Houten, J. *Inorg. Chem.* **1988**, *27*, 648. (b) Caspar, J. V.; Westmoreland, T. D.; Allen, G. H.; Bradley, P. G.; Meyer, T. J.; Woodruff, W. H. *J. Am. Chem. Soc.* **1984**, *106*, 3492. (c) Smothers, W. K.; Wrighton, M. S. *J. Am. Chem. Soc.* **1983**, *105*, 1067. (d) Kober, E. M.; Meyer, T. J. *Inorg. Chem.* **1982**, *21*, 3967. (e) Forster, M.; Hester, R. E. *Chem. Phys. Lett.* **1981**, *81*, 42. (f) Bradley, P. G.; Kress, N.; Hornberger, B. A.; Dallinger, R. F.; Woodruff, W. H. *J. Am. Chem. Soc.* **1981**, *103*, 7441. (g) Braterman, P. S.; Harriman, A.; Heath, G. A.; Yellowlees, L. J. *J. Chem. Soc., Dalton Trans.* **1983**, 1801. (h) Carlin, C. M.; DeArmond, M. K. *Chem. Phys. Lett.* **1982**, *89*, 297.

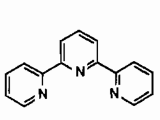

1

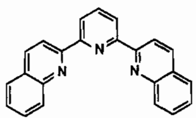

2

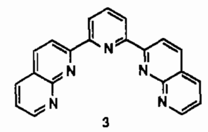

3

complexes. One explanation for these observations is that MLCT for terpyridine complexes is made up of components associated with the central and distal aza-aromatic rings of the ligand. For complexes of **2** and **3**, the shorter wavelength portion of the absorption band might be associated with the central pyridine ring and the longer wavelength component with the more electronegative distal rings. For the tpy complex both the central and distal rings are pyridines, leading to the more narrow and intense absorption at shorter wavelength.

This conclusion is supported by our earlier observations with Ru(II) complexes of a series of 3,3′:5′,3″-bis(polymethylene)-bridged derivatives of tpy.[8] We found that increasing nonplanarity of the ligand had only a small effect on the energy or intensity of the MLCT absorption. This observation would be consistent with partially localized metal-to-ligand interactions for the central and distal pyridine rings of these ligands where delocalization of charge favored by resonance interaction would be less important. Efforts to interpret the absorption spectra of mixed-ligand Ru(II) complexes involving tpy would also be clarified by this theory.[10]

To further investigate the nature of the MLCT state for tpy complexes we have studied the series of ligands **4**, which incorporate a para-substituted 4′-phenyl substituent. The nature of the substituent R has been varied to span a range of electron-donating and -withdrawing groups. These systems were prepared according to a simple two-step procedure in which para-substituted benzaldehydes are used to form the central pyridine ring of the ligand.[6] Analogous unbridged systems **5** were prepared by the classical Chichibabin reaction[7] and served to assess the importance of conformation on the 4′-phenyl substituent. Ruthenium(II) complexes of **4** and **5** were prepared in a straightforward manner.

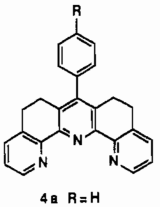

4a R = H
b R = CH_3
c R = Cl
d R = NMe_2
e R = NO_2

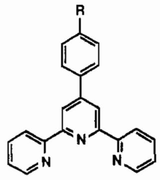

5a R = H
b R = CH_3
c R = Cl

The NMR spectra of $Ru(\mathbf{4})_2^{2+}$ and $Ru(\mathbf{5})_2^{2+}$ are characteristic of a meridional orientation of the ligands and were readily interpreted in the manner described earlier,[9] and the data are summarized in Table I. Noteworthy is the fact that within both series of complexes, involving **4** or **5**, the proton resonances for H_2–H_5 are almost invariant, indicating that the electronic environment of the distal pyridine rings is insensitive to changes in the substituent R. The incorporation of a 5,3′-dimethylene bridge causes H_4 to shift downfield about 0.3 ppm. On the other hand, the proton chemical shifts of the 4′-phenyl substituent are quite sensitive to the nature of R, as evidenced by the differences for H_o and H_m between $Ru(\mathbf{4d})_2^{2+}$ and $Ru(\mathbf{4e})_2^{2+}$.

The electronic spectra of the ruthenium complexes were obtained as 5×10^{-5} M solutions in CH_3CN. The long-wavelength (MLCT) absorption bands for the complexes of **4b–e** are depicted in Figure 3. The complexes of **4b,c,e** all absorb at the same wavelength, while the dimethylamino complex **4d** absorbs at about 5 nm longer wavelength. More sensitive to the electronic nature of R is the intensity of the absorption band. We observe the most intense peak for the system where R is most electron withdrawing (R = NO_2) and the weakest band where R is most electron donating (R = NMe_2). The other two complexes involving **4b** and **4c** are intermediate in the expected order.

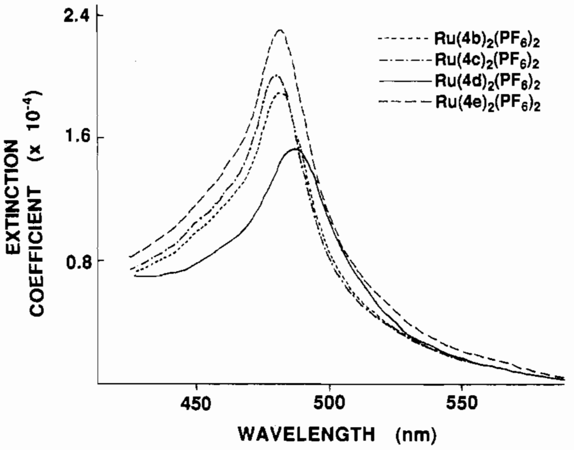

Figure 3. Electronic absorption spectra of bridged bis(para-substituted-4′-phenylterpyridyl)ruthenium(II) complexes (5×10^{-5} M in CH_3CN).

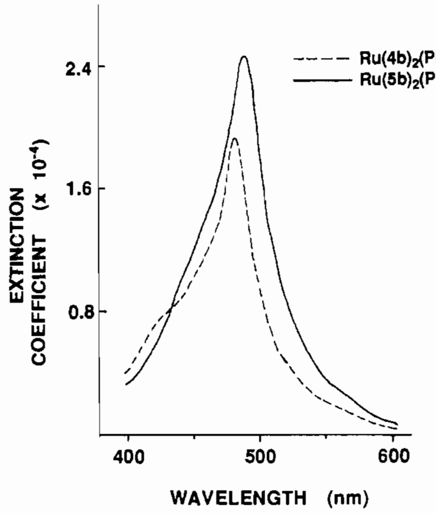

Figure 4. Electronic absorption spectra of bridged vs unbridged bis(4′-*p*-tolylterpyridyl)ruthenium(II) complexes (5×10^{-5} M in CH_3CN).

Upon examination of a molecular model of these systems, we reasoned that the phenyl proton ortho to the terpyridyl unit would interact with the bridge methylene unit to force the 4′-phenyl ring to become nearly orthogonal to the chelating moiety. Thus, we prepared the series $Ru(\mathbf{5})_2^{2+}$, where the steric inhibition to resonance between the phenyl and terpyridine moieties should be diminished. The electronic spectrum for $Ru(\mathbf{5b})_2^{2+}$ is representative of the series and is shown in Figure 4 along with that of the corresponding bridged complex. We observe a more intense, lower energy absorption for the unbridged system, indicating better resonance interaction between the 4′-phenyl ring and the central pyridine ring. Although the difference in absorption maxima is only 9 nm, the envelope for the $Ru(\mathbf{5b})_2^{2+}$ absorption is appreciably larger. This observation is in accord with the greater mobility of the 4′-phenyl ring leading to the accessibility of more vibrational levels for the MLCT state.

Table II presents the half-wave redox potentials for the ruthenium complexes of **4** and **5**. All the waves were quasi-reversible in DMSO. Oxidation of the dimethylamino group and reduction of the nitro group interfered with measurement of the corresponding potentials for these systems. Once again, clear and significant differences due to substituent effects are observed, but their actual magnitude is relatively small.

For the bridged systems, $Ru(\mathbf{4})_2^{2+}$, the oxidation and reduction potentials each span a range of only 20–40 mV. The ordering for the complexes of **4b,c,e** is not quite as expected, but the differences are never more than 20 mV. The extreme cases are clearly consistent: $Ru(\mathbf{4a})_2^{2+}$ shows the most negative reduction potentials, while $Ru(\mathbf{4d})_2^{2+}$ shows the most positive oxidation.

For the unbridged systems, the substituent effects are more clearly evident. All these systems reduce with more ease than

---

[10] Berger, R. M.; McMillan, D. R. *Inorg. Chem.* **1988**, *27*, 4245.

Table II. Half-Wave Potentials for Ruthenium(II) Complexes[a]

complex	R	oxidn	redn	
$Ru(\mathbf{4a})_2^{2+}$	H	+1.27 (140)	−1.21 (90)	−1.46 (100)
$Ru(\mathbf{4b})_2^{2+}$	CH_3	+1.26 (135)	−1.22 (85)	−1.46 (90)
$Ru(\mathbf{4c})_2^{2+}$	Cl	+1.26 (145)	−1.23 (110)	−1.48 (115)
$Ru(\mathbf{4d})_2^{2+}$	NMe_2	*b*	−1.25 (75)	−1.49 (85)
$Ru(\mathbf{4e})_2^{2+}$	NO_2	+1.28 (140)	−0.90 (185)[c]	
$Ru(\mathbf{5a})_2^{2+}$	H	+1.26 (170)	−1.15 (75)	−1.37 (80)
$Ru(\mathbf{5b})_2^{2+}$	CH_3	+1.24 (165)	−1.18 (160)	−1.42 (165)
$Ru(\mathbf{5c})_2^{2+}$	Cl	+1.29 (150)	−1.12 (110)	−1.34 (120)

[a] Potentials are given in volts vs SCE for 0.002 M DMSO solutions, 0.1 M in TBAP, recorded at 25 ± 1 °C. The difference between cathodic and anodic peak potentials (mV) is given in parentheses. [b] Oxidation of the NMe_2 group interferes with this process. [c] This value represents reduction of the NO_2 group, which obscured reduction of the metal center.

their bridged analogues and in the expected order $Ru(\mathbf{5c})_2^{2+} > Ru(\mathbf{5a})_2^{2+} > Ru(\mathbf{5b})_2^{2+}$ for both the first- and second-reduction couples. This same ordering is found for oxidation, where the influence of bridging appears to be less pronounced.

The results outlined above are consistent with our premise that the MLCT state for terpyridine complexes of Ru(II) has separate components associated with the central and distal pyridine rings of the ligand. As we change the electron-withdrawing ability of the para substituent on a 4′-phenyl ring, the energy of absorption is affected only to a small degree, while the effectiveness (intensity) of MLCT varies by a factor of about 1.5 between the extremes of **4d** and **4e**. As resonance interaction of the 4′-phenyl ring is improved by elimination of the 3,3′:5′,3″-bridges, absorption energy again remains relatively invariant, but the absorption envelope widens slightly toward longer wavelength.

Although the introduction of 4- and 4″-substituents onto terpyridine is synthetically more challenging, we are working along these lines to examine the influence of substituents on the distal rings of these complexes.

Acknowledgment. Financial support from the Robert A. Welch Foundation and the National Science Foundation (Grant CHE-8607935) is gratefully acknowledged. The NMR spectrometer was partially funded by the NSF (Grant CHE-866352). We thank Professor D. Klassen for a generous gift of $Ru(biq)_3(ClO_4)_2$, Y. Wang for assistance, and one of the reviewers for helpful comments.

Contribution from the Chemical Physics Program,
Washington State University, Pullman, Washington 99164-4620

An Update of Pseudoplanar, Bibridged $Cu_nX_{2n+2}^{2-}$, $Cu_nX_{2n+1}L^-$, and $Cu_nX_{2n}L_2$ Oligomer Stacking Patterns: Structure of 1,2-Dimethylpyridinium Bis(μ-chloro)trichloroaquadicuprate(II)

Marcus R. Bond and Roger D. Willett*

Received November 2, 1988

Many copper(II) halide compounds occur as pseudoplanar, bibridged oligomeric species with formula $Cu_nX_{2n+2}^{2-}$, $Cu_nX_{2n+1}L^-$, or $Cu_nX_{2n}L_2$ ($X = Cl^-$, Br^-; L = neutral ligand). Within the oligomer the copper ions are four-coordinate and approximately planar with adjacent Cu ions linked by two bridging ligands. The Cu(II) ion frequently completes its coordintion sphere by forming longer, axial (semicoordinate) bonds to halide ions in neighboring, coplanar oligomers, thus forming stacks. Semicoordinate bond formation between oligomers requires a relative displacement of neighboring oligomers that varies periodically along the stack. The surprising variety of stacking patterns was recently tabulated by Geiser and co-workers.[1] The purpose of this note is to update this table of known stacking patterns and to report the structure of an $ACu_2Cl_5(H_2O)$ compound exhibiting an unusual stacking pattern.

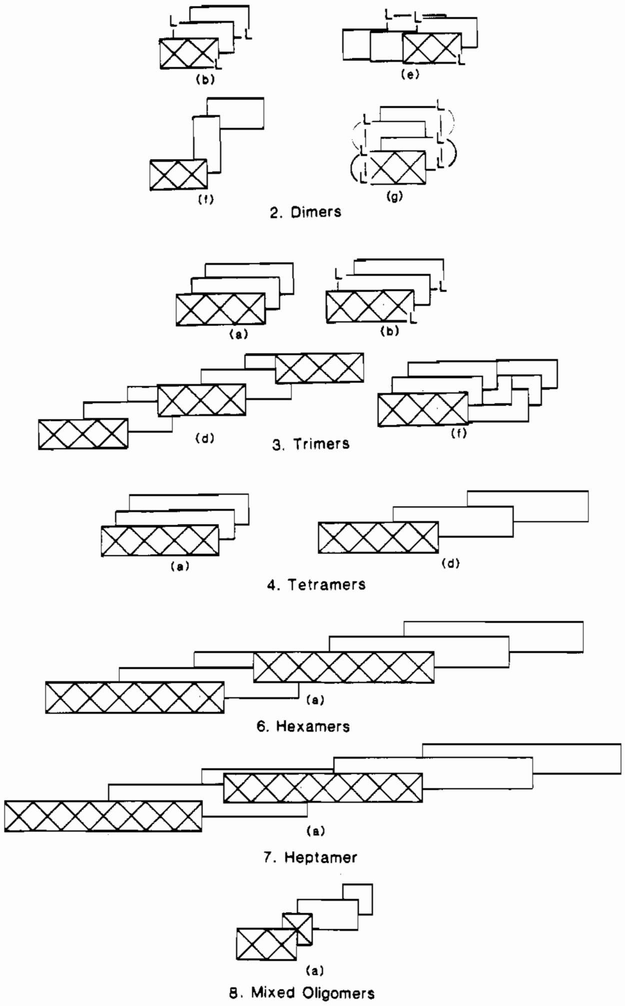

Figure 1. Envelope stacking pattern diagrams (cf. Table I).

Stacking Pattern Notation

Symbols for the various stacking patterns are devised by using the following procedure.[1] (1) The oligomer is idealized as a planar, rectangular envelope with the ligands located on the perimeter, the copper ions located in the interior, all copper–ligand distances equal, and all ligand–Cu–ligand angles either 90 or 180°. (2) The envelopes are stacked with displacements of neighboring envelopes mimicking observed oligomer displacements. (3) A stacking symbol of the form $n(m_\parallel, m_\perp, \phi)$ is constructed with the terms defined as follows: n, the number of copper ions in the oligomer; $m_\parallel d$ and $m_\perp d$, the translational displacement of the envelope taken parallel and perpendicular to the Cu–Cu axis (d = ligand–ligand distance along an edge); and ϕ, rotation of the envelope about the normal to the envelope plane. As many parenthetic symbols are concatenated as are necessary to describe the repeat unit of the stack.

It is necessary to add the following rules: (3a) $m_\parallel d$ and $m_\perp d$ are the displacements necessary to move the *central point* of one oligomer atop the *central point* of its neighbor; (4) the rotation axis is always taken through the central point; and (5) if an oligomer belongs to more than one stack, then the full symbol consists of a concatenation of the individual symbols (enclosed in brackets) for each possible stack preceded by n. Rule 3a guarantees that mixed oligomer stacking patterns will be unique, except for a uniform change of sign in $m_\parallel$ or $m_\perp$ (the value of n that most closely precedes the parenthetic symbol denotes the

---

[1] Geiser, U.; Willett, R. D.; Lindbeck, M.; Emerson, K. *J. Am. Chem. Soc.* **1986**, *108*, 1173.

0020-1669/89/1328-3267$01.50/0